Journal of Theoretical and Applied Mechanics, Sofia, 2012, vol. 42, No. 4, pp. 19–30

BUCKLING OF BEAMS AND COLUMNS UNDER COMBINED AXIAL AND HORIZONTAL LOADING WITH VARIOUS AXIAL LOADING APPLICATION LOCATIONS

Amir Javidinejad
Zodiac Aerospace,
7330 Lincoln Way, Garden Grove, CA USA,
e-mail: amir.javidinejad@gmail.com

[Received 09 August 2012. Accepted 05 November 2012]

Abstract. In this paper the buckling behaviour of an I-beam under combined axial and horizontal side loading is examined. It is to shown that the actual application location of the axial loading governs the buckling behaviour of the long I-beam. Theoretical formulation is developed to determine the critical buckling load for such combined loading configuration from the elastic static theory. Both, the beam deflection theoretical model and the critical load capacity are derived for this combined loading condition. The Finite Element Analysis (FEA) is utilized to apply the axial load on the beam at various configuration locations and it is shown that this application location determines the buckling behaviour and the critical load of the buckling of the I-beam. Numerical example is given.
Key words: Buckling, Finite Element Analysis (FEA), horizontal side load, elastic buckling.

1. Introduction

Various sources are available in the field of elastic stability theory that derive the equations necessary for determining the critical buckling load of a beam or column while under axial loading [1,2,3], or torsion loading [4]. However, there are not many or rarely you will find sources that discuss buckling under applied moment or a horizontally side loading in combination to an axial loading.

The elastic stability solutions normally account for critical buckling load of the beam or column under axial loading, where the application of the load is along the longitudinal axis of the structure. In this paper, a solution for combined loading of both axial and horizontal side load is developed. In

this solution, the loading is considered to be directly at the centre of the cross section of the beam or column. A horizontal side loading is applied to the beam or column at a distance from axial loading.

Now, it is not trivial to develop a solution that accounts for the axial loading to be applied and distributed evenly over the cross-section of the beam or column tip. Finite element models are built for this reason and investigated to examine the buckling mode of the beam or column under 1) a concentrated load at the exact centre of the beam or column cross-section, 2) axial loading applied to the four corners of the cross-section evenly and 3) axial loading applied to the four corners and the exact centre of the beam cross-section. In all three cases, a side loading is applied at a distance away from the beam tip.

Also, the beam is considered to be pinned in one end and pinned and restrained from any horizontal movement and free from any vertical movements at the other end where the axial loading is applied. It is to conclude from the finite element analysis investigation that the mode and behaviour of buckling is governed by these type of axial load applications and not the horizontal side loading applied. In the following section the theory and constraint configuration of the beam under investigation is elaborated on, in details.

2. The Calculation of Critical Load and Deflection

Consider the column loaded with a combination of axial and bending (horizontal side) loads as shown in the following Fig. 1.

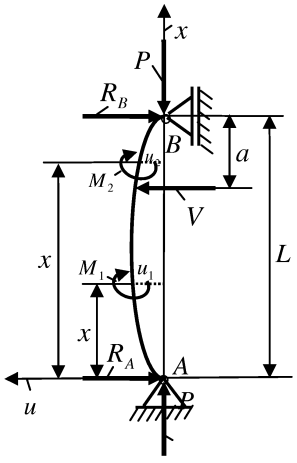

Fig. 1. The column buckling under combined loading.

The equation representing the bending of the column is,

$$EI\frac{d^2u}{dx^2} = -M. \tag{1}$$

By virtue of simple elastic static theory the lateral reactions at the points A and B are, $R_A = \dfrac{Va}{L}$ and $R_B = \dfrac{V(L-a)}{L}$, respectively. Using these reaction loads, one can develop the total bending moment along the axis of the column as [5],

$$M_1 = Pu_1 + \frac{Vax}{L} \quad \text{for} \quad 0 \le x \le L-a, \tag{2}$$

and

$$M_2 = Pu_2 + \frac{V(L-a)(L-x)}{L} \quad \text{for} \quad L-a \le x \le L. \tag{3}$$

Now, by substituting the moment equations (2) and (3) into the expression (1), one would have,

$$EI\frac{d^2u_1}{dx^2} = -Pu_1 - \frac{Vax}{L} \quad \text{for} \quad 0 \le x \le L-a, \tag{4}$$

$$EI\frac{d^2u_2}{dx^2} = -Pu_2 - \frac{V(L-a)(L-x)}{L} \quad \text{for} \quad L-a \le x \le L. \tag{5}$$

As before, by introduction of the term,$k^2 = \dfrac{P}{EI}$, the available solutions for these differential equation are,

$$u_1 = u_1(x) = c_1\cos kx + c_2\sin kx - \frac{Vax}{PL} \quad \text{for} \quad 0 \le x \le L-a, \tag{6}$$

$$u_2 = u_2(x) = c_3\cos kx + c_4\sin kx - \frac{V(L-a)(L-x)}{PL} \quad \text{for} \quad L-a \le x \le L. \tag{7}$$

For this system by applying the applicable boundary conditions that are known as these shown before,

$$u_1(A) = u_1(0) = 0,$$

$$u_2(A) = u_2(0) = 0,$$

$$u_1(L-a) = u_2(L-a), \tag{8}$$

$$\frac{du_1(L-a)}{dx} = \frac{du_2(L-a)}{dx},$$

the constants of the integration c_1, c_2, c_3 and c_4 are determined as,

$$c_1 = 0, \tag{9}$$

$$c_2 = \frac{V \sin ka}{Pk \sin kL}, \tag{10}$$

$$c_3 = \frac{V \sin k(L-a)}{Pk}, \tag{11}$$

$$c_4 = -\frac{V \sin k(L-a)}{Pk \tan kL}. \tag{12}$$

By substitution of the above constants into expressions (6) and (7) one would have the following final deflection expressions for the column,

$$u_1 = \frac{V \sin ka}{Pk \sin kL} \sin kx - \frac{Va}{PL}x \quad \text{for} \quad 0 \le x \le L-a, \tag{13}$$

$$u_2 = \frac{V \sin k(L-a)}{Pk \sin kL} \sin k(L-x) - \frac{V(L-a)(L-x)}{PL} \quad \text{for} \quad L-a \le x \le L. \tag{14}$$

It is known, that the maximum lateral displacement occurs in the middle of the column where, $x = \dfrac{L}{2}$. Thus, using the expressions (13) and (14), for the maximum displacement one would have, (for $a = \dfrac{L}{2}$):

$$u\left(x = \frac{L}{2}\right) = \frac{V \sin^2 k\dfrac{L}{2}}{Pk \sin kL} - \frac{VL}{4P}. \tag{15}$$

We know that the expression (15) goes to infinity at $\sin kL = 0$. Thus, the first term solution is,

$$kL = \pi, \tag{16}$$

which, by substitution of the k term, would produce the critical axial load for buckling of the column as,

$$\sqrt{\frac{P_{cr}}{EI}} = \frac{\pi}{L} \quad \text{or} \quad P_{cr} = \frac{\pi^2 EI}{L^2}. \tag{17}$$

3. Numerical Analysis

For numerical analysis an I-beam of length 2.032 m (80 inches) is selected. The beam has a web of 0.254 m (10 inches) and a flange of 0.102 m (4 inches); with web and flange thickness of 0.010 m (0.4 inches). This beam cross-section dimensions produce a moment of inertia of $I = 1.80\text{E-}6$ m^4 (4.315 in^4). A plot of the beam length versus the produced critical buckling load is generated in the Fig. 2 following. The beam is under combined axial and side bending loading. The critical buckling load for a 2.032 m (80 inches) long beam with the preceding cross-section is determined to be about 293,004 N (65,870 pounds) by using the expression (17).

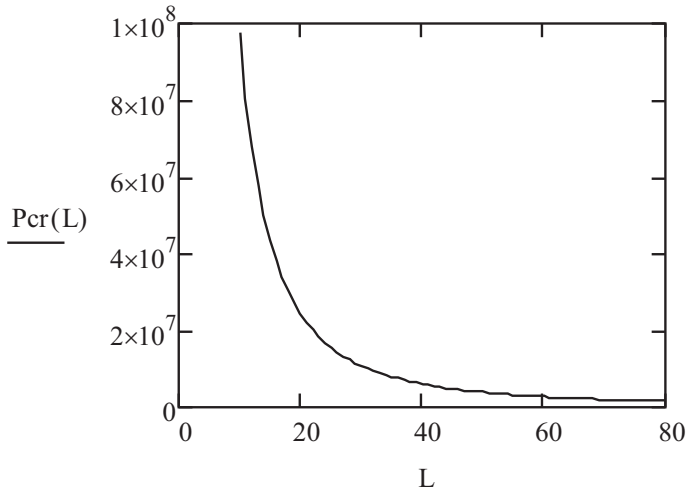

Fig. 2. The beam length vs. critical buckling load.

In Fig. 2 above the length "L" is in inches and the critical buckling load "Pcr" is in pounds force. Later it would be shown in the Finite Element section that, the side loading is creating a resistance for the beam to buckle in its "natural" horizontal positive "x" direction, hence raising the critical buckling load for the combined loading case.

4. Finite Element Analysis

An FEA model was built and the various loading configurations were investigated for verification of the theoretical results. For analysis, a beam of 2.032 m (80 inches) long with an I cross-section was modelled. The beam has a web of 0.254 m (10 inches) and a flange of 0.102 m (4 inches); with web and flange thickness of 0.01 m (0.4 inches). The Fig. 3 illustrates the I-beam cross section and the FEA mesh of the beam model. The mesh is a fine mesh with minimum element size that is in the same order of the web and flange thickness. Also adequate number of elements is selected in the beam length direction to avoid any under-estimation of the results. The Fig. 3 is showing a partial of the beam length.

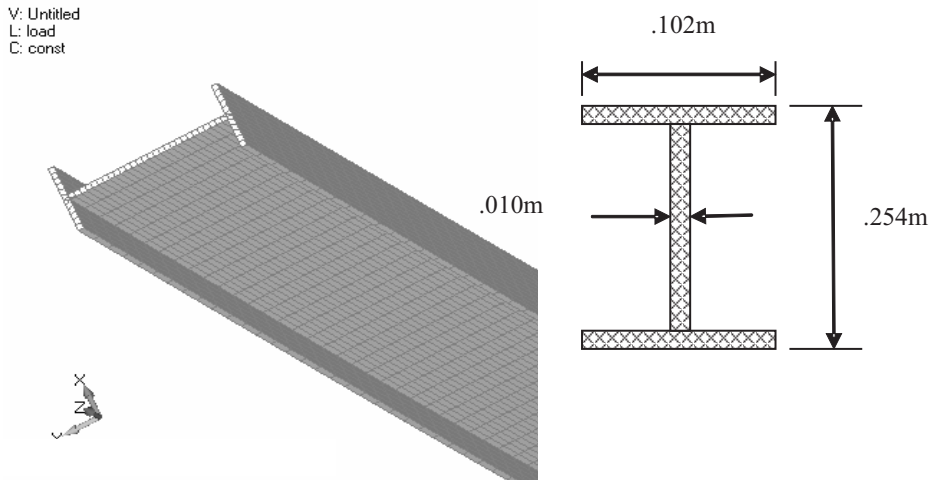

Fig. 3. The Beam Cross-Section and FEA Mesh

The axial load was applied to the beam from the top normal to the beam cross-section and the horizontal bending load was applied from the side of the beam at 0.762 m (30 inches) down from the beam tip. The axial loading was applied to the beam cross-section in three different ways to investigate the effects of the load application location on the beam buckling behaviour and mode. The following Fig. 4 illustrates the different axial load configuration on the beam cross-section. Figure 4(a) shows the axial load being applied exactly to the centre of the beam cross-section. Hereby, refer to this configuration as "a-loading" type. Figure 4(b) shows application of the axial load to four corners of the beam with the same previous load divided into four equal loads. Hereby, refer to this configuration as "b-loading" type.

Finally, Fig. 4(c) shows the axial being divided into five equal loads and applied to the four corners and the centre of the beam cross-section. Hereby, refer to this configuration as "c-loading" type. This is used to show the importance of the load application location in the buckling problem. How the axial loading is applied to the beam and column would make a great difference in both the buckling critical load and the behaviour of the buckling section.

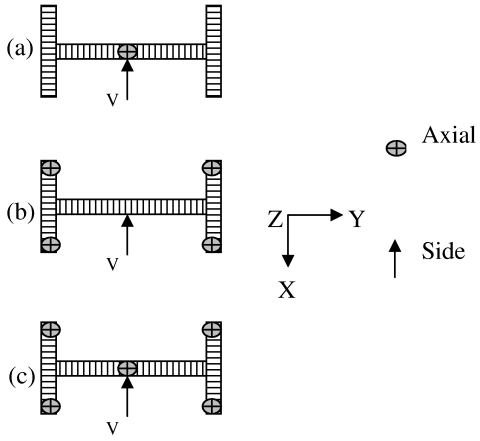

Fig. 4. The three different loading configurations

A net axial load of 44,482 N (10,000 pounds) and a horizontal side load of 22,241 N (5,000 pounds) were applied to the beam cross section. A buckling load FEA analysis was ran and the following critical buckling eigenvalues which translate to critical buckling load was determined.

Figure 5(a) following shows buckling results for the type "a-loading" configuration. The eigenvalue determined is 6.332. Since the applied axial load is 44,482 N (10000 pounds) for this model, the critical buckling load would be the applied axial load times the eigenvalue; which gives a critical buckling load of 281,661 N (63,320 pounds). Notice, the deformation contour illustrates that the beam buckles in the direction of the applied side bending load.

The maximum deflection is also determined to be at the location where the actual horizontal side loading is applied to the beam. This is the same location at which the beam would be buckling at. Note, the deflection contour is only showing the displacement under the applied load and not the actual critical buckling load. For determination of the buckling mode displacement refer to expressions (13) and (14) in the theoretical calculations section of this paper in preceding sections.

Fig. 5(a). Type "a-loading" configuration FEA results

Fig. 5(b). Type "a-loading" configuration FEA results without side loading

Theoretically the same beam without the side loading should have similar and same critical buckling load. Fig. 5(b) illustrates the validity of this theory via numerical methods as shown by the similar eigenvalue.

The following Fig. 6(a) is the FEA buckling results for the type "b-loading" configuration. The eigenvalue determined is 10.225. This gives a critical buckling load of 454,830 N (102,250 pounds) for the same beam, which

Fig. 6(a). Type "b-loading" configuration FEA results

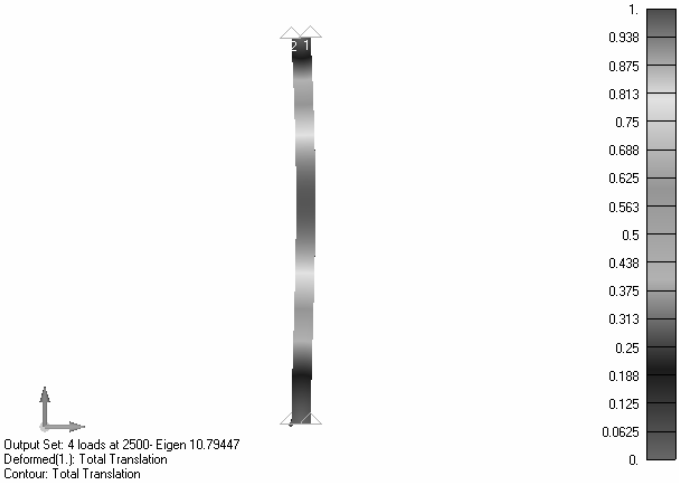

Fig. 6(b). Type "b-loading" configuration FEA results without the side loading

is higher that type "a-loading" configuration. Notice that the buckling of the beam is in the opposite direction of the applied horizontal side load. The redistribution of the axial loading (type "b-loading") is making a difference in the buckling behaviour of the beam. It appears, that this loading configuration is producing the natural positive "x" direction buckling, which is also expected from a beam loaded axially only.

The following Fig. 7(a) is the FEA buckling results for the type "c-loading" configuration. The eigenvalue determined is 10.230. This gives a critical buckling load of 455,053 N (102,300 pounds) for the same beam, which is again higher that type "a-loading" configuration but equal to the type "b-loading". Notice that the buckling of the beam is again in the opposite direction of the applied horizontal side load. The redistribution of the axial loading (type "c-loading") is making a difference in the buckling behaviour of the beam as well.

Fig. 7(a). Type "c-loading" configuration FEA results

Fig. 7(b). Type "c-loading" configuration FEA results without the side loading

Similarly, for this type "b-loading" without the side loading the critical buckling load is similar and same as the beam with the side loading as shown by the similar eigenvalue determined in Fig. 6(b).

Likewise, for the type "c-loading" without the side loading the eigenvalue determined via finite element numerical methods is similar and the same as the beam with side loading as shown in Fig. 7(b).

It can safely be conculuded that type "a-loading" with the entire axial load concentrated exactly at the center of the beam cross-section is accurately matching the theoretical results presented in section 3 of this paper. The other loading configurations add an about 42% load to the final critical buckling load.

It should be understood that the changes in the loading application location configuration contributes into the instability of the beam or column inversely. That is a higher critical buckling load that can be achieved by re-distributing the load at the tip of the beam or column. This theory is clear from the finite element analysis of such beams but yet it would be of great interest to experimentally investigate this phenomena as well.

5. Conclusion

The buckling of the beams under combined loading of the axial and side bending loads was investigated. A theoretical calculation of the critical buckling load was developed. Three separate axial load application configurations for the same beam under combined loading were investigated and simulated by finite element analysis methods. The eigenvalues and the critical buckling loads were determined. It was concluded that the re-distribution of the axial load on the tip of the beam raises the critical buckling load of the beams. It also effects the buckling mode direction of the maximum buckling location. The beams were also analyzed without the side loading to further prove that the three "end-tip" loading type configurations are the actual driving factor in determining the critical buckling loads.

REFERENCES

[1] Brush, D. O., B. O. Almorth. Buckling of Bars, Plates and Shells, USA, New York, NY, McGraw-Hill, 1975.

[2] Chen, W. F., E. M. Lui. Structural Stability: Theory and Implementation, PTR Prentice Hall, 1987.

[3] Timoshenko, S. P., J. Gere. Theory of Elastic Stability, 1961.

[4] Hsiao, K. M., H. H. Chen, C. C. Lin. Lateral-torsional Buckling Analysis of Doubly Symmetric Thin-walled Beam under Axial Force and Bending Moment. *Advances in Structures*, (2003), 496–500.

[5] Bruhn, E. F. Analysis and Design of Flight Vehicle Structures, 1973.